The EMBO Journal vol.8 no.11 pp.3235-3244, 1989

Molecular basis of functional diversity of voltage-gated potassium channels in mammalian brain

Walter Stühmer, Johann Peter Ruppersberg[1], Klaus Hasso Schröter[1], Bert Sakmann[1], Martin Stocker[2], Karl Peter Giese[2], Astrid Perschke[2], Arnd Baumann[2,3] and Olaf Pongs[2]

Max-Planck-Institut für biophysikalische Chemie, Abteilung Membranbiophysik, D-3400 Göttingen, [1]Max-Planck-Institut für medizinische Forschung, Abteilung Zellphysiologie, D-6900 Heidelberg and [2]Ruhr-Universität Bochum, Lehrstuhl für Biochemie, D-4630 Bochum, FRG

[3]Present address: Zentrum für Molekulare Neurobiologie, Hamburg, D-2000 Hamburg 20, FRG

Communicated by B.Sakmann

Cloning and sequencing of cDNAs isolated from a rat cortex cDNA library reveals that a gene family encodes several highly homologous K^+ channel forming (RCK) proteins. Functional characterization of the channels expressed in *Xenopus laevis* oocytes following microinjection of *in vitro* transcribed RCK-specific RNAs shows that each of the RCK proteins forms K^+ channels that differ greatly in both their functional and pharmacological properties. This suggests that the molecular basis for the diversity of voltage-gated K^+ channels in mammalian brain is based, at least partly, on the expression of several RCK proteins by a family of genes and their assembly to homooligomeric K^+ channels with different functional properties.

Key words: channel diversity/gene family/mammalian brain/potassium channels

Introduction

Potassium (K^+) channels are ubiquitous in membranes of both excitable and inexcitable cells (Hille, 1984; Latorre *et al.*, 1984; Lewis and Cahalan, 1988). A major function of K^+ channels is to set the membrane potential and thereby regulate the electrical excitability of the cell. K^+ channels are exceptionally diverse in their conductance and gating mechanisms, and most cells express several subtypes of K^+ channels that are characterized by different functional and pharmacological properties (Moczydlowski *et al.*, 1988; Rudy, 1988).

Voltage-dependent K^+ currents are important for shaping the action potential and can be broadly subdivided into practically non-inactivating 'delayed' $I_{K(V)}$ and rapidly inactivating 'transient' $I_{K(A)}$ outward currents (Hille, 1984). Single-channel current recordings have revealed that both delayed and transient K^+ currents are mediated by several subtypes of channels, which share some functional properties (Marty and Neher, 1985; Hoshi and Aldrich, 1988a,b). This raises the question of the molecular distinction between the functional subtypes of K^+ channels.

Knowledge about the molecular structure of voltage-dependent K^+ channels has been considerably advanced by the analysis of cloned cDNAs encoding K^+ channel forming proteins from *Drosophila melanogaster* (Jan and Jan, 1989) and from mammalian brain (Baumann *et al.*, 1988; Tempel *et al.*, 1988). An extensive homology between *Drosophila* and rodent brain K^+ channel proteins was observed at the level of derived amino acid sequences (Baumann *et al.*, 1988; Kamb *et al.*, 1988; Pongs *et al.*, 1988; Schwarz *et al.*, 1988; Tempel *et al.*, 1988; Christie *et al.*, 1989; McKinnon, 1989) although the functional properties were rather different (Stühmer *et al.*, 1988; Christie *et al.*, 1989). Therefore it might be inferred that relatively small variations in amino acid sequences of channel forming proteins would be responsible for the diversity of voltage-gated K^+ channels in mammalian neurones.

We have now cloned several cDNAs that encode proteins belonging to a gene family and are expressed in rat brain (RCK proteins). The amino acid sequences of the RCK proteins were derived from cDNAs isolated from a library of rat brain cortex and the functional properties of the channels formed by the RCK proteins were measured after injection of the respective RCK-specific RNA into *Xenopus laevis* oocytes. Each RCK protein assembles into oligomeric voltage-activated K^+ channels with functional and pharmacological characteristics for a particular RCK protein. Thus K^+ channel diversity in rat brain is due to a family of genes that encode several highly homologous proteins. These proteins assemble to form functional K^+ channels that differ in their voltage-dependent gating mechanism, channel conductance and toxin binding properties.

Results

Characterization of structurally related potassium channel subunits in rat brain

Recently, we have characterized a rat brain cDNA named RCK1 (Baumann *et al.*, 1988), which expresses K^+ channels after nuclear injection into *X.laevis* oocytes (Stühmer *et al.*, 1988). The channels exhibit gating properties similar to those of non-inactivating delayed rectifier K^+ channels in mammalian neurones. The gene expressing the RCK1 channel is apparently present only once in the haploid rat genome. When Southern blots of rat genomic DNA were probed with cDNA RCK1 under conditions of low stringency (Baumann *et al.*, 1988), additional hybridizing restriction fragments were detected. We have hybridized, with an RCK1 cDNA probe, a rat cortex cDNA library under conditions of low stringency and have screened for other cDNAs encoding RCK1 related proteins.

Several hybridizing clones were isolated and sequenced. The clones encoded three additional K^+ channel subunits (RCK3, RCK4 and RCK5 respectively). As an example, the combined RCK4 nucleotide and deduced amino acid

©IRL Press

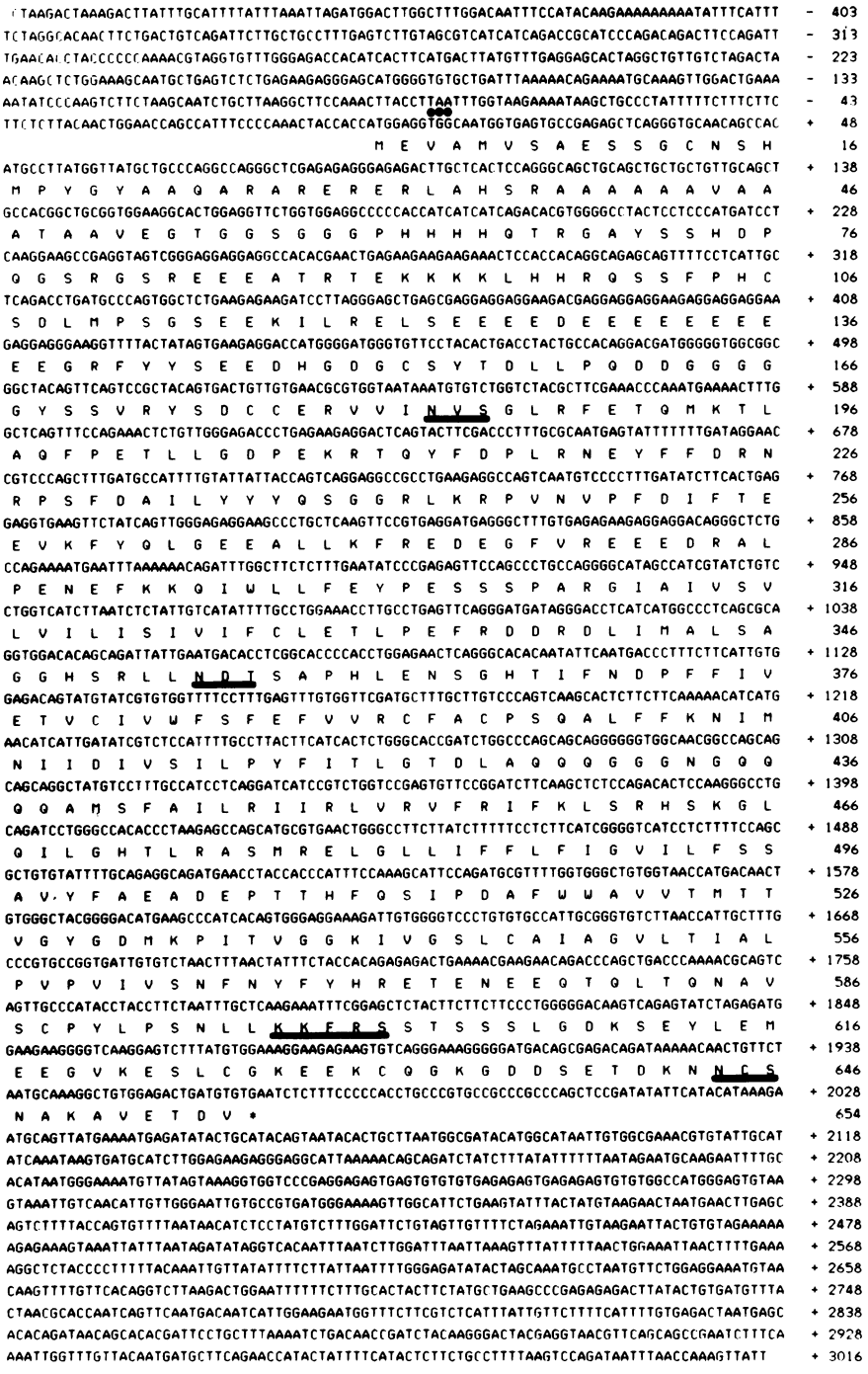

Fig. 1. DNA sequence and predicted amino acid sequence of the rat cortex K^+ channel forming protein RCK4. Nucleotides are numbered in the 5′−3′ direction, beginning with the first residue of the ATG triplet encoding the methionine initiation site. The nucleotides on the 5′ side of residue 1 are indicated by negative numbers. The number of the nucleotide residue at the right end of each line is given. The deduced amino acid sequence code (in one-letter code) is shown below the nucleotide sequence. Amino acid residues are numbered beginning with the methionine initiation site. Numbers of the last residues are given on the right-hand side. The non-sense codon TGA at the end of ORF is marked by an asterisk. The putative N-glycosylation and phosphorylation sites are indicated by bars. Dots denote the first upstream in frame stop codon in the 5′-untranslated sequence. The sequence presented is a composite of several overlapping cDNA clones. The sequence of cDNA clone R521 was from nucleotide −492 to +1783, that of cDNA clone R611 from nucleotide +1094 to +2248, and that of cDNA clone R2a from nucleotide +1578 to +3015.

sequence is shown in Figure 1. The sequence is 3507 nucleotides long. It lacks most of the 5′- and 3′-untranslated sequences of the corresponding poly(A^+) RNA. The deduced RCK4 protein sequence consists of 655 amino acids residues and has a calculated mol. wt of 73 398. The RCK4 sequence contains three potential N-glycosylation sites (Asns 183, 354 and 644 in Figure 1) and one potential cAMP-dependent phosphorylation site (Krebs and Beavo, 1979) (Ser 601). The RCK4 sequence is very similar to that of RCK1 protein (Figure 2). The overall sequence identity is 59%. The most obvious difference between RCK1 and RCK4 protein is that the amino terminal ends do not match, that of RCK4 protein being considerably longer.

The amino acid sequences of proteins RCK3 and RCK5

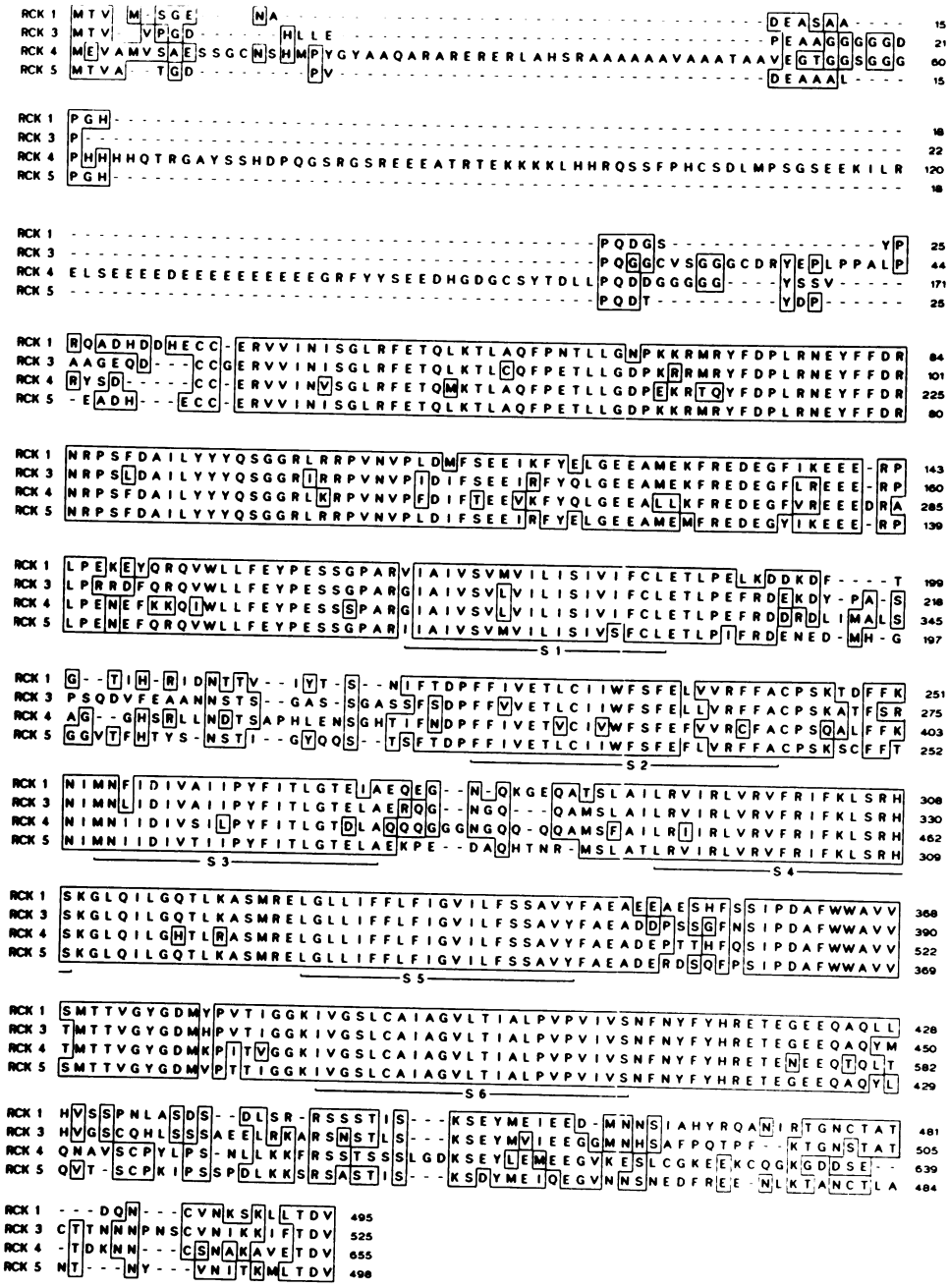

Fig. 2. Sequence homologies of deduced rat cortex K^+ channels (RCK proteins). Identical sets of amino acid residues are enclosed with solid lines. Gaps (−) have been introduced for maximal alignment of RCK sequences. Proposed transmembrane segments S1−S6 are indicated by brackets. Termini of each segment are tentatively assigned on the basis of hydropathy profiles shown in Figure 3. The RCK1 sequence is from Baumann *et al.*, 1988. The cDNA sequence called RCK2 is not listed because it is identical to the RCK1 sequence as published previously (Baumann *et al.*, 1988). The RCK3 sequence is deduced from RCK3 cDNA. The nucleotide sequence is 2460 nucleotides long. The RCK5 sequence is deduced from a composite, 2406 nucleotide long cDNA sequence. The sequence of cDNA R821 was from nucleotide 1 to 1821, that of cDNA R4a was from nucleotide 145 to 2406. The cDNA sequences have been submitted to the EMBL data bank.

derived from the two other cDNAs, were remarkably similar to that of RCK1 protein (Figure 2). Its sequence identity with RCK3 and RCK5 was 84 and 72% respectively. The deduced RCK3 protein sequence consists of 525 amino acids and has a calculated mol. wt of 58 397. The RCK5 sequence consists of 498 amino acids and has a calculated mol. wt of 56 768. The RCK3 sequence contains two potential N-glycosylation sites (Asns 59, 229) and the RCK5 sequence five potential N-glycosylation sites (Asns 38, 207, 465, 480 and 490) which conform with the consensus sequence NXT/S for N-glycosylation. Most of the N-glycosylation sites are located at analogous positions in the four RCK proteins (Figure 2). The potential cAMP-dependent phosphorylation sites (Krebs and Beavo, 1979) (Ser 470 in RCK3 and Ser 448 in RCK5 protein) are also located at positions similar to the ones in RCK4 and RCK1 protein.

The architecture of the deduced RCK proteins apparently obeys common structural principles as revealed by a comparative analysis of the hydropathy profiles (Kyte and Doolittle, 1982) of the four deduced RCK proteins

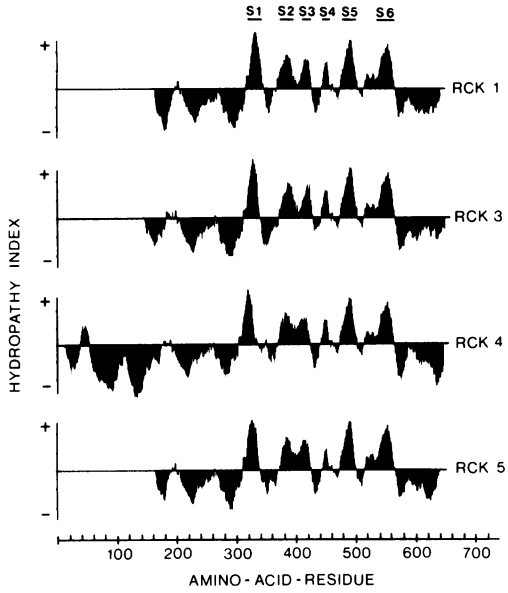

Fig. 3. Hydropathy profiles of RCK proteins. Profiles were computed with a window size of 19 amino acids (Kyte and Doolittle, 1982). Positive index values indicate hydrophobic groups. Proposed transmembrane segments S1–S6 are indicated by solid bars.

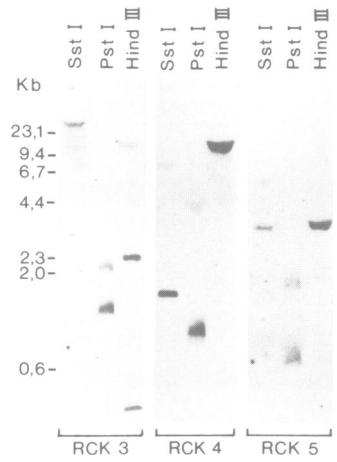

Fig. 4. Southern analysis of genomic DNA with RCK cDNA. Rat genomic DNA was digested with the restriction enzymes *Sst*I, *Pst*I and *Hin*dIII. Restriction fragments were separated by electrophoresis in 0.7% agarose gels. Southern blots were hybridized under conditions of high stringency with ^{32}P-labelled RCK cDNA probes. RCK probes are indicated at the bottom. Probes were for RCK4-cDNA clone R521 and for RCK5-cDNA clone R4a. DNA of phage cI857 Sam 7 digested with *Hin*dIII was used as size marker as indicated on the left hand side.

(Figure 3). This analysis predicts that the RCK proteins include six hydrophobic, possibly membrane-spanning, segments. They have been designated S1–S6 as indicated in Figures 2 and 3 by analogy to the proposed models for the voltage-dependent sodium (Noda *et al.*, 1984) and the *Shaker* K^+ channels (Pongs *et al.*, 1988). These models orient the six proposed transmembrane segments S1–S6 in a pseudosymmetric fashion across the membrane such that the amino and carboxyl termini are located on the cytoplasmic side and that the amino acid sequences joining segments S1 and S2, S3 and S4, and S5 and S6 are located on the extracellular side. The sequences of the proposed transmembrane segments S1–S4 of the RCK proteins are highly conserved, those of segments S5 and S6 are identical. If amino acid substitutions between Met, Leu, Ile and Val are regarded as conservative (Dayhoff *et al.*, 1978), then only four non-conservative amino acid substitions occur among the sequences of the RCK hydrophobic segments S1–S4. These substitutions are Ile-Ser (RCK5 segment S1), Leu-Phe and Phe-Cys (RCK4 segment S2), and Ile-Phe (RCK1 segment S3) (Figure 2). In addition, sequences which face the intracellular side of the membrane according to the proposed topology have been highly conserved. Most notably, 104 out of the 135 amino acids that precede the hydrophobic segments of RCK proteins are identical in all four RCK sequences and 99 are identical between the four RCK sequences and the *Drosophila Shaker* K^+ channels (Kamb *et al.*, 1988; Pongs *et al.*, 1988; Schwarz *et al.*, 1988). Only 13 non-conservative amino acid substitutions have occurred between these sequences in rat brain as compared to *Drosophila* K^+ channel subunits. The alignment of the amino acid sequences of RCK proteins and the comparison of the hydropathy profiles show that RCK proteins share a core region with almost identical sequences. Only sequences in the core region that join the proposed membrane-spanning segments S1/S2 and S3/S4 at the extracellular side of the membrane have not been conserved. The core region is flanked by variant amino and carboxy terminal ends. The variations are more pronounced in the amino- than in the carboxy-terminal sequences of RCK proteins.

Rat cortex potassium channel subunits belong to a gene family

The family of voltage-sensitive K^+ channels of the *Shaker* locus of *Drosophila* is encoded in one large transcription unit (Kamb *et al.*, 1988; Pongs *et al.*, 1988; Schwarz *et al.*, 1988). It is expressed into diverse mRNAs encoding variant $I_{K(A)}$-channel subunits (Iverson *et al.*, 1988; Timpe *et al.*, 1988a,b). The mRNAs are produced by alternative transcription and splicing mechanisms from one gene. Consequently, diversity is generated in the *Shaker* K^+ channel family by variant amino- and carboxy-terminal ends which flank a constant core region. Diversity is created similarly in the RCK protein family. The latter, however, shows also sequence variations in the core region. These variations are more pronounced at the nucleic acid than at the amino acid sequence level. This excludes the possibility that the different cDNA sequences are generated by alternative splicing of the primary transcript. Therefore, RCK proteins are not encoded in one gene like *Shaker*, but belong to a gene family similar to the transmitter-gated ion channels. Members of this gene family apparently are present only once in the haploid rat genome. This notion is supported by hybridizing RCK3, RCK4 and RCK5 cDNA probes to a Southern blot of rat genomic DNA digested with various restriction enzymes (Figure 4). Southern blot experiments with RCK1 cDNA as probe have previously been published (Baumann *et al.*, 1988). Each RCK cDNA probe hybridized at high stringency to a few, but different restriction fragments of rat genomic DNA. Therefore, we conclude that RCK1, RCK3, RCK4 and RCK5 proteins are expressed from different single copy genes.

Functional expression of homomeric RCK channels in Xenopus laevis oocytes

The functional and pharmacological properties of the channels formed by the various RCK proteins were

Table I. Functional characteristics of channels expressed in *Xenopus* oocytes following injection of a single RCK specific RNA

mRNA type	Selectivity	Activation			Inactivation			Single-channel currents
	dV/D (mV)[a]	$V^{n1/2}$ (mV)[b]	a_n (mV)[c]	t_n (ms)[d]	$V^{h1/2}$ (mV)[e]	a_h (mV)[f]	t_h (%)[g]	i (0) (pA)[h]
RCK1	57(1)	−29.7 ± 7 (7)	− 6.5 ± 1.8 (7)	15.5 ± 4.4 (5)	−47.0 ± 1.4 (2)	4.1 ± 0.5 (2)	83.4 ± 6 (7)	0.87 (3)
RCK3	61(2)	−25.2 ± 7 (7)	− 6.6 ± 1.9 (7)	13.7 ± 6.5 (9)	−44.7 ± 4.2 (3)	16.0 ± 3.2 (3)	14.4 ± 6 (5)	0.96 (3)
RCK4	53(1)	−21.7 ± 7 (5)	−16.9 ± 3 (5)	3.2 ± 0.8 (8)	−73.6 ± 5.4 (5)	12.8 ± 2.2 (5)	<2 (10)	0.47 (3)
RCK5	55(1)	−34.3 ± 9.7 (5)	− 4.5 ± 1.3 (5)	6.3 ± 1.8 (6)	−44.8 (1)	5.6 (1)	60.0 ± 21 (5)	1.02 (4)

Numbers in parenthesis refer to number of experiments.
[a]Refers to change in reversal potential in mV for a 10-fold change in extracellular K^+ concentration. Whole-cell current recording.
[b]Refers to test potential in mV where the conductance increase has reached one-half of its maximal value. The conductance was calculated for each test potential by dividing the current amplitude by the driving force. The potassium reversal potential was assumed to be −100 mV. Ensemble current recording from macro-patches. Voltage steps were made from −80 mV holding potential.
[c]Refers to slope of normalized conductance−voltage relation. Its value corresponds to the change in test potential (in mV) to cause an e-fold increase conductance.
[d]Refers to rise time of ensemble patch currents in ms. It was measured at 0 mV test potential following step changes from −80 mV membrane potential. The rise time refers to the time the current rises from 10 to 90% of its final value.
[e]Refers to prepulse membrane potential in mV at which the current response to a step to 0 mV test potential is 50% of its maximal value. Prepulse duration is 25 s. Holding potential −80 mV. Ensemble currents from macro-patches. In oocytes expressing RCK1 and RCK5 channels the currents do inactivate over periods of several minutes. The value given is for a prepulse duration of 25 s, which may not reflect the true steady-state equilibrium potential for inactivation.
[f]Refers to slope of steady-state inactivation (h_∞) curve. Change in prepulse membrane potential (in mV) necessary to cause an e-fold reduction in the size of the response to a test pulse to 0 mV.
[g]Refers to ratio of peak amplitude to amplitude at the end of a 3.2 s voltage pulse at 0 mV test potential. Holding potential was −80 mV. For oocytes expressing RCK4 channels the average decay time constant was 109 ± 58 ms (n = 10).
[h]Refers to single-channel current amplitude in pA at 0 mV membrane potential. The respective chord conductances, assuming a reversal potential of −100 mV are 8.7, 9.6, 4.7 and 10.2 pS respectively.

characterized after microinjection of cRNAs derived from RCK cDNAs into *X.laevis* oocytes. Functionally expressed K^+ channels were characterized by recording membrane currents in response to depolarizing voltage steps and measuring their reversal potentials, their voltage-dependent activation and inactivation properties and their single-channel current amplitude.

The ion selectivity of the functionally expressed RCK channels was determined by measuring the reversal potential of tail currents in various extracellular solutions when Na^+ was replaced partially by K^+ in the range of 5−100 mM K^+, as described in Stühmer *et al.* (1988). The shift in reversal potential with increasing K^+ concentration was consistent with the assumption that all RCK channels are highly selective for K^+ over Na^+ or Cl^- (Table I). The kinetics of the RCK3 channel were greatly affected by the extracellular potassium concentration as has been shown previously in squid axon K^+ channels (Stühmer and Conti, 1979; Swenson and Armstrong, 1981).

To measure their time course and voltage dependence, ensemble K^+ currents were recorded from macro-patches in the cell-attached recording configuration of the patch clamp technique (Stühmer *et al.*, 1987). Figure 5A illustrates the voltage-dependent activation of outward currents mediated by RCK1, RCK3, RCK4 and RCK5 channels in response to steps in membrane voltage to various depolarizing test potentials. Each family of curves was recorded from a different oocyte previously injected with a particular RCK-specific RNA. Following the voltage steps, the K^+ current begins to rise in a voltage-dependent manner. At 0 mV test potential it reaches its maximum within a few milliseconds and then remains either on a plateau (RCK1, RCK3, RCK5) or begins to decay (RCK4) during the 50 ms test pulse.

Figure 5B shows the normalized conductance−voltage [G/G_{max} (V)] relations of the four RCK channels for the peak responses. The currents mediated by RCK1, RCK3 and RCK5 channels activate at comparable test potentials of −45 to −30 mV and saturate at 30−40 mV. The conductances are half-maximal in the range of −26 to −33 mV (Table I). Also, the voltage dependence of activation of these channels is similar (Table I). In contrast, the current mediated by RCK4 channels activates at more negative potentials (~ −55 mV) and the slope of the conductance−voltage relation is much shallower (Table I). The activation time courses, measured at 0 mV test potential, vary between 3 and 15 ms in the different RCK channels (Table I).

The inactivation of the currents mediated by the different RCK channels also shows characteristic differences. The steady-state half-inactivation voltage as well as the slopes of the steady-state inactivation curves differ considerably between RCK1, RCK3, RCK5 channels and RCK4 channels (Table I). Figure 6 illustrates the pronounced differences in inactivation time courses. During voltage steps of 3.2 s the current mediated by RCK1 and RCK5 channels inactivates by less than one-half, whereas the current mediated by RCK3 and RCK4 are inactivated by >80%. All RCK channels inactivate completely during test pulses lasting several minutes. This indicates that inactivation is characterized by more than one decay time constant, the faster component showing pronounced differences in amplitude (Table I) and decay time constant.

Single-channel currents which were recorded in response

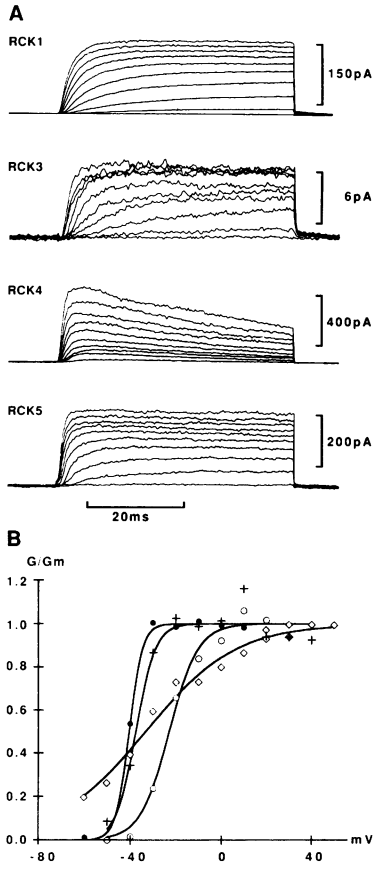

Fig. 5. Conductance–voltage relations of RCK channels. (**A**) Families of outward currents in response to depolarizing voltage steps. From top to bottom RCK1, RCK3, RCK4, RCK5. The traces are responses to 50 ms voltage steps from −50 to 40 mV in 10 mV intervals. Ensemble currents recorded from macro-patches. Sampling at 10 kHz, filtering at 3 kHz low pass. (**B**) Plots of normalized conductance (G/G_m) versus test potential for different RCK channels (RCK1: open circles; RCK3: crosses; RCK4: diamonds; RCK5: filled circles). To obtain the conductance values the current at a particular test potential was divided by the driving potential assuming a reversal potential of −100 mV. The lines showed the results of a non-linear least-squares fit of a Boltzmann isotherm (see Materials and methods) to the conductance values. The maximal conductance (G_m) obtained by the fit was used to normalize the data. The half-activation voltages in this plot are −24 mV (RCK1), −37 mV (RCK3), −30 mV (RCK4) and −40 mV (RCK5).

to voltage steps from −60 to 0 mV are shown in Figure 7. The step size of elementary currents at 0 mV varied between 0.46 pA (RCK4) and 1.02 pA (RCK5). The single channel current–voltage relations were measured in cell attached patches with normal frog Ringer's solution on the extracellular side. For all channels, the current–voltage relation is linear in the voltage range −20 to 20 mV. However, since this is a rather narrow range for conductance estimation, we measured the average amplitudes at 0 mV membrane potential. While the RCK1, RCK3 and RCK5 channels have rather similar single-channel current amplitudes, that of the RCK4 channel is considerably lower (Table I).

Pharmacology of RCK channels

A profile of the pharmacological sensitivity of the different RCK channels to the K^+ channel blockers 4-aminopyridine (4-AP) and tetraethylammonium (TEA) and several basic peptide toxins was determined. The concentration

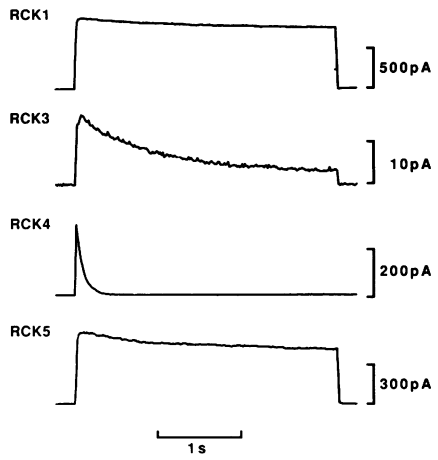

Fig. 6. Inactivation time course of currents mediated by different RCK channels. Ensemble currents from macro-patches recorded at 0 mV test potential from oocytes expressing RCK1, RCK3, RCK4 and RCK5 channels at 0 mV test potential. Duration of the test pulse was 3.2 s. Holding potential was −80 mV. Note difference in the degree of inactivation at the end of the 3.2 s pulse. Sampling at 62.5 Hz and low pass filtering at 120 Hz.

dependence of the block of outward currents by a particular substance was determined in whole-cell current recordings at 20 mV test potential and the results are summarized in Table II. A striking difference in the inhibition of K^+ currents by TEA is observed between channels formed by RCK1 and RCK5 proteins. The RCK4 channels have a lower sensitivity to 4-AP than the other RCK channels. Both slowly inactivating channels, RCK1 and RCK5, are much more sensitive to DTX than the inactivating channels RCK3 and RCK4. A different profile is observed for CTX, which blocks RCK1, RCK3 and RCK5 well, but is much less effective on RCK4 channels.

Discussion

Comparison between K^+ channels in neurones and RCK channels expressed in Xenopus oocytes

An important question resulting from the molecular and functional diversity of RCK proteins is their relation to K^+ channels in native membranes. To establish the molecular identity of a K^+ channel in its native cell membrane and a particular RCK channel expressed in *Xenopus* oocytes, properties such as the voltage and time dependence, the single-channel amplitude and the susceptibility to blockers should be compared. This comparison assumes that the K^+ channels expressed in oocytes accurately reflect the functional properties of K^+ channels in the native membrane. This has not yet been shown and only preliminary conclusions can be drawn on the molecular structure of K^+ channels in native membranes.

Delayed K^+ outward currents which inactivate only slowly, on a time-scale of hundreds of milliseconds, are found in neurones of different origins (Hille, 1984). Non-inactivating outward currents, e.g. in PC12 cells or frog spinal cord, are mediated by channels with a low (5–15 pS) channel conductance (Harris *et al.*, 1988; Hoshi and Aldrich, 1988a,b). Low conductance non-inactivating K^+ channels which are DTX sensitive were found in rat sensory neurones (Feltz and Stansfeld, 1988). Non-inactivating K^+ channels which are DTX sensitive participate in regulating transmitter

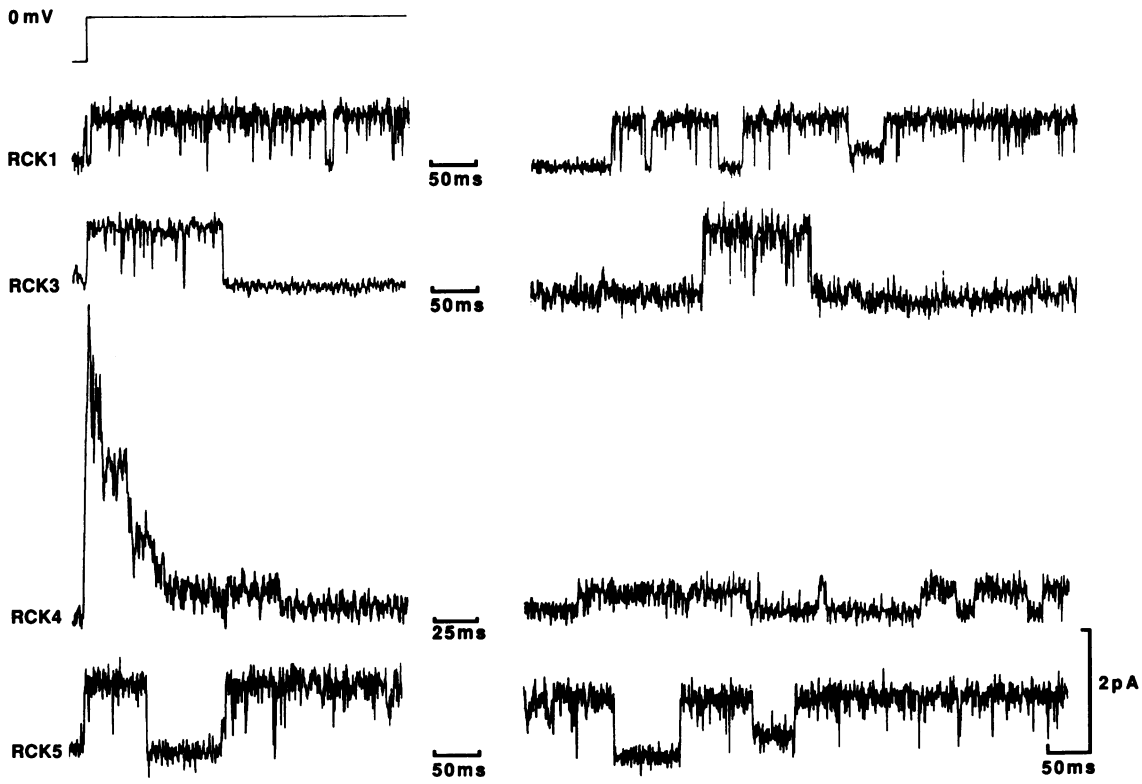

Fig. 7. Differences in the conductance of channels formed by different RCK proteins. Single-channel currents recorded from membrane patches of oocytes injected with different RCK-specific RNAs. From top to bottom RCK1, RCK3, RCK4 and RCK5 channels. The left side shows traces of currents recorded in response to voltage steps from −60 to 0 mV. Time course of the voltage step is shown above the traces. The right side shows traces of currents recorded during prolonged depolarization of the patch to 0 mV. Records are from different patches than those shown on the left side. Time-scale is the same for all traces except for the trace marked RCK4 on the left part. Amplitude calibration refers to all traces. Upward deflection corresponds to channel opening. Note transient opening of RCK3 and RCK4 channels and long-lasting opening of RCK1 and RCK5 channels. Sampling at 2 kHz, low pass filtering at 1 kHz.

release (Dreyer and Penner, 1987). K^+ channels formed by RCK1 and RCK5 proteins are practically non-inactivating in the time range of hundreds of milliseconds, they are of low conductance and they are blocked by nanomolar concentrations of DTX. This may indicate that RCK1 and RCK5 proteins constitute the low conductance subclass of non-inactivating, DTX-sensitive K^+ channels in the cell body and the endings of peripheral and central mammalian neurones.

Transient K^+ outward currents which inactivate in tens of milliseconds are also mediated by a variety of channels (Hille, 1984). In most mammalian neurones the channels which mediate rapidly inactivating currents have a conductance of 15−20 pS (Kasai *et al.*, 1986; Hoshi and Aldrich, 1988a,b). Fast inactivating K^+ currents mediated by low conductance (5 pS) channels have only been found in medulloblastoma cells (Ruppersberg *et al.*, 1988). The RCK3 and RCK4 channels show some of the functional characteristics of channels mediating transient $I_{K(A)}$ type currents in neurones, in particular their inactivation properties. However, the single channel conductance of RCK3 and RCK4 channels is lower than those of $I_{K(A)}$-channels in neurones and they are not sensitive to DTX as found for brain $I_{K(A)}$-channels (Halliwell *et al.*, 1986). Thus homomeric RCK3 and RCK4 channels may be expressed in medulloblastoma cells but the molecular nature of the rapidly inactivating channels with 15−20 pS conductance present in mammalian neurones remains to be elucidated. The recent observation that $I_{K(A)}$-type currents are observed in oocytes injected with fractionated mRNA only if two different size fractions of poly(A^+) mRNA were injected (Rudy *et al.*, 1988) may indicate that the neuronal $I_{K(A)}$ channels are formed by different subunits. The RCK4 protein could be one of the constituent subunits.

Table II. Pharmacological characteristics of RCK channels expressed in *Xenopus* oocytes

mRNA species	4-AP (mM)	TEA (mM)	DTX (nM)	MCDP (nM)	CTX (nM)
RCK1	1.0	0.6	12	45	22
RCK3	1.5	50	>600	>1000	1
RCK4	12.5	>100	>200	>2000	>40
RCK5	0.8	129	4	175	6

Numbers in this table refer to ID_{50} values (50% inhibition of peak current), measured at 20 mV test potential; all experiments made with whole-cell current recording.

Structural implications

Voltage-dependent gating which is accompanied by a gating current has been correlated with the structure of the proposed transmembrane segment S4 (Noda *et al.*, 1984, 1986; Tanabe, 1987; Pongs *et al.*, 1988). This segment is present in virtually all voltage-sensitive channels and consists of the sequence motif Lys/Arg-X-X, repeated 4−8 times (X being a hydrophobic amino acid). It has been suggested that it is the S4 segment which renders an ion channel voltage

sensitive. A decrease in the density of positive charges (i.e. the number of Lys/Arg-X-X repeats) of S4 segments of the Na^+ channel correlates with a decrease in the slope of the voltage dependence of activation (Stühmer *et al.*, 1989). A popular model is that the movement of charges caused by a voltage-dependent translocation of the S4 segment constitutes the gating current (Catterall, 1988; Guy, 1988). A comparison of the normalized conductance–voltage relations of the various RCK channels (Figure 5B) indicates that the voltage-dependence of activation for RCK4 channels is less pronounced than that of RCK1, RCK3, and RCK5 channels respectively. However, the sequences of the S4 segments are identical among the RCK proteins apart from one Ile/Val amino acid exchange (Figure 2) which does not alter the charge on the S4 segment. Thus the charge alone cannot be the sole determinant for the steepness of the voltage-dependence of activation of K^+ channels formed by RCK proteins.

The alignment of the deduced RCK protein sequences (Figure 2) and that of RCK1 protein with the *Drosophila Shaker* sequence (Baumann *et al.*, 1988) showed that the central region of these K^+ channel proteins has been highly conserved over >600 million years. The highly conserved structures of the voltage-dependent K^+ channels presumably participate in important and specific functions, e.g. the formation of a K^+ selectivity filter and the physical gate. The conserved central region of the RCK proteins is interspersed with highly variable stretches of amino acid sequences (Figure 2), mainly in the bend regions between the proposed transmembrane segments S1 and S2, S3 and S4, and S5 and S6 respectively. Following the proposed orientation of the membrane-spanning segments across the membrane (Pongs *et al.*, 1988), these variable bend regions of the RCK channel proteins are located on the extracellular side. By analogy to what has been found for the pore formed by the acetylcholine receptor channel (Imoto *et al.*, 1988), rings of negative charges being near the mouth of the RCK channel are probably important for K^+ transport rates. Therefore, the absence of negatively charged amino acid side chains in the S2–S3 bend region of RCK4 protein may explain why RCK4 channels have a lower conductance than the other RCK channels.

The affinity of the positively charged toxins DTX and CTX, which block K^+ channels from the outside, should also depend on the number and kind of negatively charged amino acids being near or in the mouth of the K^+ channel. Accordingly, K^+ channels which are DTX sensitive should have in the S1–S2, S3–S4 and/or S5–S6 bend regions an acidic amino acid residue that is not found at the equivalent position in DTX-insensitive channels. We have searched the amino acid sequences that face the extracellular side in the proposed topology of *Shaker* and RCK proteins for the presence or absence of distinct glutamic and aspartic acid residues. The results suggest that the reduced DTX sensitivity of *Shaker*, RCK3 and RCK4 channels may be due to a replacement of Glu 353 (RCK1) and, respectively, of Asp 354 (RCK5) in the S5–S6 bend region by uncharged amino acids. The pharmacological characteristics of RCK channels expressed in *Xenopus* oocytes (Table II) indicate that RCK channels have variant affinities to the K^+ channel blockers DTX, MCDP and CTX respectively. This observation is comparable with previous biochemical work. Both equilibrium and kinetic measurements of radioiodinated DTX binding showed that two populations of DTX acceptors, associated with neuronal K^+ channels, were discernible in preparations of chick synaptic membranes (Black and Dolly, 1986) and of rat brain membranes (Rehm and Lazdunski, 1988). The two DTX-acceptor subtypes bind β-bungarotoxin either with high or low affinity. Only the latter subtype appears to be sensitive to MCDP also (Rehm and Lazdunski, 1988; Rehm *et al.*, 1988). Although the RCK1 channel is sensitive to DTX and MCDP, but not to β-bungarotoxin (Stühmer *et al.*, 1988), it is still a matter of conjecture whether and how the biochemically characterized toxin-acceptors are related to the RCK1 and RCK5 K^+ channel proteins.

Since its discovery, CTX has been widely used to block Ca^{2+}-activated K^+ channels (Moczydlowski *et al.*, 1988). Recent studies have shown that CTX also blocks voltage-activated K^+ channels (MacKinnon *et al.*, 1989; Sands *et al.*, 1989; Schweitz *et al.*, 1989). Similarly, our data indicate that DTX-sensitive as well as insensitive K^+ channels are blocked by nanomolar concentrations of CTX. A comparison of the RCK1, RCK3 and RCK5 sequences with the one of RCK4, which expresses a CTX-insensitive K^+ channel, suggests that the number of acidic amino acid residues in the S3–S4 bend region could correlate with the affinity of the RCK channels to CTX. This correlation would predict that the CTX insensitivity of RCK4 channels is due to replacement of acidic residues by glutamines immediately adjacent of the carboxy-terminal end of proposed transmembrane segment S3. It has been proposed that Ca^{2+}- and voltage-activated K^+ channels have a homologous CTX-binding domain (MacKinnon *et al.*, 1989; Schweitz *et al.*, 1989). The sequence of the S3–S4 bend regions is quite variable among RCK proteins. Therefore, the CTX-binding function common to Ca^{2+}- and voltage-activated K^+ channels cannot presently be exploited to predict a similarity in sequence between these two classes of K^+ channels.

Molecular basis of K^+ channel diversity

Two molecular principles have been discovered so far as the basis of voltage-sensitive K^+ channel diversity. In the case of the *Shaker* protein family, diversity is generated by multiple alternative splicing of a large primary transcript into a family of variant mRNAs. In the case of the RCK proteins family described here, the diversity is generated by the expression of variant RCK genes which were apparently derived from a common ancestor gene. Recently, the *Shaker* protein family has been extended by additional members (Butler *et al.*, 1989). However, the genes *Shab, Shaw* and *Shal* have a homology which is not as extensive as that of RCK to *Shaker* proteins (the sequence identity of the integral membrane portion is ~50%). Thus, K^+ channel diversity could result from the expression of an extended gene family, as well as from alternate splicing of primary transcripts. Our earlier proposition that members of the *Shaker* family form homo- or heteromultimeric structures, possibly also with components coded in other parts of the *Shaker* complex or even outside of it (Pongs *et al.*, 1988) offers yet another molecular basis for the great diversity of K^+ channels. This raises the possibility that RCK proteins form heteromultimeric structures. The assembly of such structures could increase dramatically the possible number of functionally diverse K^+ channels derived from the RCK gene family.

Materials and methods

Screening of rat brain cDNA library

A rat brain cDNA library kindly provided by P.Seeburg (ZMBH, Heidelberg) was screened at low stringency according to Benton and Davis (1977). The hybridization was performed in 5 × SSC (20 × SSC is 3 M sodium chloride, 0.3 M sodium citrate, pH 7.0), 0.1% bovine serum albumin, 0.1% Ficoll, 0.1% polyvinylpyrollidone, 100 μg/ml denatured salmon sperm DNA, 50 mM sodium phosphate (pH 7.0), 0.1% SDS, 43% deionized formamide at 37°C for 12 h (McGinnis *et al.*, 1984). Filters were washed twice in 2 × SSC, 0.1% SDS for 5 min at room temperature, followed by two washes for 15 min each at 42°C. The probe was a labelled fragment from RCK1 cDNA (Pongs *et al.*, 1988). Recombinant DNA was propagated in ER1 host-vector system under L2 containment conditions, as defined in the guidelines of the Federal German Government for recombinant DNA research. Recombinant DNA was isolated according to Maniatis *et al.* (1982). ^{32}P-labelled DNA probes were prepared with an oligonucleotide labelling kit (Boehringer).

Southern blots

Restriction enzyme-digested genomic DNA was separated on 0.7% agarose gels and transferred to nitrocellulose (Schleicher and Schüll, Dassel, FRG). Prehybridization was in 50% deionized formamide, 5 × SSC, 100 μg/ml denatured salmon sperm DNA, 4 × Denhardt's solution, 0.1% SDS for 10 min at 42°C. Hybridization was in the same buffer containing 1 × 10^6 c.p.m./ml ^{32}P-labelled probes for 20 h at 42°C. Washing was in 1 × SSC, 0.1% SDS for 5 min at room temperature, then twice for 30 min in 0.2 × SSC, 0.1% SDS at 65°C. Hybridization to Southern blots of restriction fragments of recombinant phages were done without formamide at 65°C. Blots were washed as above.

Restriction maps and sequencing

Restriction maps were derived by a combination of complete, single and double digests followed by gel electrophoresis of the resulting fragments on 0.7% agarose gels (Maniatis *et al.*, 1982). cDNAs were subcloned into Bluescript and deletions were generated with DNase I according to Lin *et al.* (1985). Deleted subclones were selected after plasmid minipreparation, restriction digestions and agarose gel electrophoresis. The dideoxy nucleotide sequencing technique was used for sequencing both strands of overlapping cDNA subclones (Sanger *et al.*, 1977).

RNA synthesis and injection into oocytes

cRNA was prepared from cDNA as described in Stühmer *et al.* (1988). After storage at −20°C the cRNA was injected into oocytes of *Xenopus laevis* (stage Vb/VI) in portions of ~50 nl/oocyte (concentration 0.5 mg/ml). The expression of RCK channels was detectable in nearly every oocyte on the second day after injection with a maximum at days 4−6. Incubation in Barth's medium at 19°C as described by Methfessel *et al.* (1986).

Current recording and data analysis

All experiments were performed in a bathing solution containing (in mM) NaCl 115, KCl 2, $CaCl_2$ 1.8, HEPES 10 (pH 7.2). In some experiments, sodium was partly replaced by potassium or blocking substances [TEA and 4-AP (Sigma), dendrotoxin and MCDP (gift from Drs F.Dreyer and E.Habermann, Universität Giessen, FRG), charybdotoxin (gift from Dr C.Miller, Brandeis University, USA)] were added to the bathing solution.

A two-microelectrode voltage clamp was used to test for the action of the toxins and to determine the whole-cell K^+ current of each oocyte prior to patch current recording. In ~20% of the oocytes injected the current was >10 μA at 0 mV test potential. This indicated that the channel density was high enough to obtain smooth current traces in ensemble current records from macro-patches.

Patch pipettes were filled with the normal bathing solution in all experiments. Pipettes for macro-patches were made from aluminium-silicate glass and had a tip diameter of ~6 μm and a resistance of 0.5−1 MΩ. The intracellular potential was simultaneously measured by a second microelectrode to monitor the transmembrane potential across the patch. To find the area of maximal channel density the oocyte was turned around by an angle of 90° between the first three patch experiments. Stimulation and sampling was done either by PDP 11/73 or by a VME-bus computer. Leak and capacitive currents were subtracted on-line using the P/4 procedure. To determine the steady- state activation or inactivation parameters the parameters $V^{1/2}$, a and G_m of a single Boltzmann isotherm of the form: $G = G_m/\{1 + \exp[(V - V^{1/2})/a]\}$ were fitted to the peak values of a family of records. To get the conductance (G) the current values were divided by the driving potential assuming a reversal potential of −100 mV. In the case of steady-state inactivation the current values were directly inserted into the equation above.

Pipettes for single-channel recording were made from borosilicate glass and had a tip diameter of ~1 μm and resistances of 3−5 MΩ when filled with bathing solution. The single-channel current records were stored on video tape and analyzed by an interactive semi-automatic procedure. Distributions of single-channel current amplitudes were fitted by either single or sums of Gaussians.

Acknowledgements

We thank Drs F.Dreyer and E.Habermann for the generous gift of DTX and MCDP and Dr C.Miller for the generous gift of CTX as well as T.Verdoorn and F.Edwards for reading the manuscript. The work was supported by grants and the Leibniz-Förderprogramm of the DFG. The sequence data will appear in the EMBL/Gen Bank/DDBJ/Nucleotide Sequence Databases under accession numbers X16001, X16002, X16003.

References

Baumann,A., Grupe,A., Ackermann,A. and Pongs,O. (1988) *EMBO J.*, **7**, 2457−2463.
Benton,W.D. and Davis,R.W. (1977) *Science*, **196**, 180−182.
Black,A.R. and Dolly,J.O. (1986) *Eur. J. Biochem.*, **156**, 609−617.
Butler,A., Wei,A., Baker,K. and Salkoff,L. (1989) *Science*, **243**, 943−947.
Catterall,W.A. (1988) *Science*, **242**, 50−61.
Christie,M.J., Adelman,J.P., Douglass,J. and North,R.A. (1989) *Science*, **244**, 221−224.
Dayhoff,M.O., Schwartz,R.M. and Orcutt,B.C. (1978) *Atlas of Protein Sequence and Structure*. National Biomedical Research Foundation, Silver Springs, MD, Vol. 5, Suppl. 3. pp. 345−352.
Dreyer,F. and Penner,R. (1987) *J. Physiol.*, **386**, 455−463.
Feltz,A. and Stansfeld,C. (1988) *J. Physiol.*, **406**, 208P.
Guy,H.R. (1988) In Agnew,W.S., Claudio,T. and Sigworth,F.J. (eds), *Molecular Biology of Ionic Channels*. Academic Press, San Diego, Current Topics in Membranes and Transport, Vol. 33, pp. 289−308.
Halliwell,J.V., Othman,I.B., Pelchen-Matthews,A. and Dolly,J.O. (1986) *Proc. Natl. Acad. Sci. USA*, **83**, 493−497.
Harris,G.L., Henderson,L.P. and Spitzer,N. (1988) *Neuron*, **1**, 739−750.
Hille,B. (1984) *Ionic Channels in Excitable Membranes*. Sinauer, Sunderland MA.
Hoshi,T. and Aldrich,R.W. (1988a) *J. Gen. Physiol.*, **91**, 73−106.
Hoshi,T. and Aldrich,R.W. (1988b) *J. Gen. Physiol.*, **91**, 107−131.
Imoto,K., Busch,C., Sakmann,B., Mishina,M., Komo,T., Nokai,J., Bujo,H., Mori,Y., Fukido,K. and Numa,S. (1988) *Nature*, **335**, 645−648.
Iverson,L.E., Tanouye,M.A., Lester,H.A., Davidson,N. and Rudy,B. (1988) *Proc. Natl. Acad. Sci. USA*, **85**, 5723−5727.
Jan,L.Y. and Jan,Y.N. (1989) *Cell*, **56**, 13−25.
Kamb,A., Tseng-Crank,J. and Tanouye,M.A. (1988) *Neuron*, **1**, 421−430.
Kasai,H., Kameyama,M., Yamaguchi,K. and Fukuda,J. (1986) *Biophys. J.*, **49**, 1243−1247.
Krebs,E.G. and Beavo,J.-A. (1979) *Annu. Rev. Biochem.*, **48**, 923−959.
Kyte,J. and Doolittle,R.F. (1982) *J. Mol. Biol.*, **157**, 105−132.
Latorre,R., Coronado,R. and Vergara,C. (1984) *Annu. Rev. Physiol.*, **46**, 485−495.
Lewis,R.S. and Cahalan,M.D. (1988) *Trends Neurol. Sci.*, **11**, 214−218.
Lin,H.C., Lei,S.P. and Wilcox,G. (1985) *Anal. Biochem.*, **147**, 114−119.
Maniatis,T., Fritsch,E.F. and Sambrook,J. (1982) *Molecular Cloning: A Laboratory Manual*. Cold Spring Harbor Laboratory Press, Cold Spring Harbor, NY.
Marty,A. and Neher,E. (1985) *J. Physiol.*, **367**, 117−141.
McGinnis,W., Levine,M.S., Hafen,E., Kuroiwa,A. and Gehring,W.J. (1984) *Nature*, **308**, 428−433.
MacKinnon,R., Reinhart,P.H. and White,M.M. (1989) *Neuron*, **1**, 997−1001.
McKinnon,D. (1989) *J. Biol. Chem.*, **264**, 8230−8236.
Methfessel,C., Witzemann,V., Takahashi,T., Mishina,M., Numa,S. and Sakmann,B. (1986) *Pflüger's Arch*, **407**, 577−588.
Moczydlowski,E., Lucchesi,K. and Ravindran,A. (1988) *J. Membrane Biol.*, **105**, 95−111.
Noda,M., Shimizu,S., Tanabe,T., Takai,T., Kayano,T., Ikeda,T., Takahashi,H., Nakayama,H., Kanaoka,Y., Minamino,N., Kangawa,K., Matsuo,H., Raftery,M.A., Hirose,T., Inayama,S., Hayashida,H., Miyata,T. and Numa,S. (1984) *Nature*, **312**, 121−127.
Noda,M., Ikeda,T., Kayano,T., Suzuki,H., Takeshima,H., Kurasaki,M., Takahashi,H. and Numa,S. (1986) *Nature*, **320**, 188−192.
Pongs,O., Kecskemethy,N., Müller,R., Krah-Jentgens,I., Baumann,A.,

Kiltz,H.H., Canal,I., Llamazares,S. and Ferrus,A. (1988) *EMBO J.*, **7**, 1087–1096.
Rehm,H. and Lazdunski,M. (1988) *Proc. Natl. Acad. Sci. USA*, **85**, 4919–4923.
Rehm,H., Bidard,J.-N., Schweitz,H. and Lazdunski,M. (1988) *Biochemistry*, **27**, 1827–1832.
Rudy,B. (1988) *Neuroscience*, **25**, 729–750.
Rudy,B., Hoger,J.H., Lester,H.A. and Davidson,N. (1988) *Neuron*, **1**, 649–658.
Ruppersberg,J.P., Spittelmeister,W., Marx,A., Siara,J., Fakler,B. and Rüdel,R. (1988) *Pflüger's Arch.*, **412**, R 16.
Sands,S.B., Lewis,R.S. and Cahalan,M.D. (1989) *J. Gen. Physiol*, **93**, 1061–1074.
Sanger,F., Nicklen,S. and Coulson,A.R. (1977) *Proc. Natl. Acad. Sci. USA*, **74**, 5463–5467.
Schwarz,T.L., Tempel,B.L., Papazian,D.M., Jan,Y.N. and Jan,L.Y. (1988) *Nature*, **331**, 137–142.
Schweitz,H., Stansfeld,C.E., Bidard,J.-N., Fagni,L., Maes,P. and Lazdunski,M. (1989) *FEBS Lett.*, **250**, 519–522.
Stühmer,W. and Conti,F. (1979) In Adam,G. and Stark,G. (eds), *A Meeting Deutsche Gesellschaft Biophysik*, Springer, New York.
Stühmer,W., Methfessel,C., Sakmann,B., Noda,M. and Numa,S. (1987) *Eur. Biophys. J.*, **14**, 131–138.
Stühmer,W., Stocker,M., Sakmann,B., Seeburg,P., Baumann,A., Grupe,A. and Pongs,O. (1988) *FEBS Lett.*, **242**, 199–206.
Stühmer,W., Conti,F., Suzuki,H., Wang,X., Noda,M., Yahagi,N., Kubo,H. and Numa,S. (1989) *Nature*, **339**, 597–603.
Swenson,R.P. and Armstrong,C.M. (1981) *Nature*, **291**, 427–429.
Tanabe,T., Takeshima,H., Mikami,A., Flockerzi,V., Takahashi,H., Kangawa,K., Kojima,M., Matsuo,H., Hirose,T. and Numa,S. (1987) *Nature*, **328**, 313–318.
Tempel,B.L., Jan,Y.N. and Jan,L.Y. (1988) *Nature*, **332**, 837–839.
Timpe,L.C., Jan,Y.N. and Jan,L.Y. (1988a) *Neuron*, **1**, 659–667.
Timpe,L.C., Schwarz,T.L., Tempel,B.L., Papazian,D.M., Jan,Y.N. and Jan,L.Y. (1988b) *Nature*, **331**, 143–145.

Received on June 20, 1989; revised on July 31, 1989